Systematic dissection of dynein regulators in mitosis

Jonne A. Raaijmakers,[1,2] Marvin E. Tanenbaum,[2,3] and René H. Medema[1,2]

[1]Department of Cell Biology, The Netherlands Cancer Institute, 1066 CX Amsterdam, Netherlands
[2]Department of Experimental Oncology and Cancer Genomics Center, University Medical Center Utrecht, 3584 CG Utrecht, Netherlands
[3]Department of Cellular and Molecular Pharmacology, University of California, San Francisco, San Francisco, CA 94158

Cytoplasmic dynein is a large minus end–directed motor complex with multiple functions during cell division. The dynein complex interacts with various adaptor proteins, including the dynactin complex, thought to be critical for most dynein functions. Specific activities have been linked to several subunits and adaptors, but the function of the majority of components has remained elusive. Here, we systematically address the function of each dynein–dynactin subunit and adaptor protein in mitosis. We identify the essential components that are required for all mitotic functions of dynein. Moreover, we find specific dynein recruitment factors, and adaptors, like Nde1/L1, required for activation, but largely dispensable for dynein localization. Most surprisingly, our data show that dynactin is not required for dynein-dependent spindle organization, but acts as a dynein recruitment factor. These results provide a comprehensive overview of the role of dynein subunits and adaptors in mitosis and reveal that dynein forms distinct complexes requiring specific recruiters and activators to promote orderly progression through mitosis.

Introduction

Cytoplasmic dynein is a large minus end–directed microtubule motor complex, involved in many different cellular processes including intracellular trafficking, organelle positioning, and microtubule organization. Mammalian cells express two cytoplasmic dynein complexes; cytoplasmic dynein 1 and cytoplasmic dynein 2. Cytoplasmic dynein 2 is mainly involved in intraflagellar transport, a process involved in the building and maintenance of cilia/flagella (Mikami et al., 2002). Unlike cytoplasmic dynein 2, cytoplasmic dynein 1 (hereafter referred to as dynein) is involved in many different processes throughout the cell cycle. Dynein is a homodimer of two heavy chains comprising a ring of six AAA domains, which binds and hydrolyzes ATP, a stalk required for microtubule binding and an N-terminal "tail." The tail of the dynein heavy chain is important for homodimerization and forms a scaffold for several noncatalytic dynein subunits. The cytoplasmic dynein 1 heavy chains (DHCs) interact with two dynein intermediate chains (DICs), four light intermediate chains (LICs) and three different light chain dimers (LL1/2, Roadblock-1/2, and TCTex1/1L; Pfister et al., 2006; Kardon and Vale, 2009).

In mitosis, dynein has been implicated in chromosome movements, spindle organization, spindle positioning, and checkpoint silencing (Sharp et al., 2000; Howell et al., 2001; Varma et al., 2008). In line with this large array of functions, dynein localizes to a variety of subcellular structures during G2 and mitosis including the nuclear envelope (NE), centrosomes, kinetochores (KTs), spindle microtubules, and the cell cortex (Pfarr et al., 1990; Steuer et al., 1990; Dujardin and Vallee, 2002; Tanenbaum et al., 2010; Kiyomitsu and Cheeseman, 2012).

The dynein motor complex interacts with multiple adaptor proteins, which are thought to be required for correct localization and activation of the complex (Kardon and Vale, 2009). The dynein activator or dynactin complex is the best characterized interactor of dynein (Gill et al., 1991; Schroer and Sheetz, 1991; Schroer, 2004). Dynactin consists of a long actin-like Arp1 filament that is capped on one site by the capping proteins CAPZA/B and interacts with the actin-related protein Arp11 and three fairly uncharacterized proteins; p25, p27, and p62 at the opposing site (Schroer, 2004). The flexible arm of the dynactin complex consists of two large p150glued subunits, which interact directly with the DICs (Vaughan and Vallee, 1995). The p150glued arm is linked to the Arp1 backbone through four

Correspondence to René H. Medema: r.medema@nki.nl

Abbreviations used in this paper: DHC, dynein heavy chain; DIC, dynein intermediate chain; KT, kinetochore; LIC, light intermediate chain; NE, nuclear envelope; NEB, nuclear envelope breakdown; SAC, spindle assembly checkpoint; STLC, *S*-trityl-L-cysteine.

The Rockefeller University Press $30.00
J. Cell Biol. Vol. 201 No. 2 201–215
www.jcb.org/cgi/doi/10.1083/jcb.201208098

p50 (dynamitin) and two p24/22 subunits (Amaro et al., 2008). p150glued can bind to microtubules directly through its CAP–Gly domain and a region containing basic amino acids (Waterman-Storer et al., 1995; Culver-Hanlon et al., 2006). The interaction of dynein with dynactin is important to link dynein to a large array of cargoes in interphase (Holleran et al., 2001; Muresan et al., 2001; Johansson et al., 2007). Furthermore, dynactin can enhance the processivity of dynein in vitro (King and Schroer, 2000; Kardon et al., 2009). Overexpression of dynamitin or a fragment of p150glued, which disrupts the interaction between dynein and dynactin, is widely used as a strategy to inhibit dynein in both interphase and mitosis (Burkhardt et al., 1997; Quintyne et al., 1999), suggesting that dynactin is indeed essential for most if not all functions of dynein (Karki and Holzbaur, 1999; Schroer, 2004). However, these approaches may have additional effects on dynein activity, therefore the role of dynactin and its subunits during cell division remains largely unknown.

Besides dynactin, dynein interacts with numerous other adaptor proteins. A complex of dynein, LIS1, and Nde1/NdeL1 promotes transport of high-load cargoes (McKenney et al., 2010). It has recently been shown that LIS1 binds to the AAA2 and AAA3 domains of the dynein motor domain and the association of LIS1 with dynein prevents the release of the microtubule-binding domain upon ATP-hydrolysis (Huang et al., 2012). This allows dynein to remain associated with microtubules for prolonged periods, which might especially be important for high-load dynein transport. Accordingly, interfering with LIS1 function results in defects in both cell migration and cell division (Kardon and Vale, 2009). Besides acting as a regulator for dynein activity, LIS1 has roles in the initiation of dynein-driven transport and in the recruitment of dynein to the NE (Egan et al., 2012; Splinter et al., 2012). LIS1 is also involved in the recruitment of dynein to MT plus ends in mammalian cells and in budding yeast (Faulkner et al., 2000; Li et al., 2005), but not other model organisms (Zhang et al., 2002; Lenz et al., 2006). The exact roles for Nde1 and NdeL1 remain controversial. Nde1 and NdeL1 have been found to both suppress and enhance the effect of LIS1 on dynein (Yamada et al., 2008; McKenney et al., 2010; Huang et al., 2012). In most cases, depletion of Nde1 or NdeL1 in cells leads to dynein inhibition-like phenotypes, although there seems to be selectivity for either Nde1 or NdeL1 in a subset of dynein-dependent processes and during different developmental stages (Vergnolle and Taylor, 2007; Zyłkiewicz et al., 2011). Furthermore, Nde1/NdeL1 have also been shown to be essential for the targeting of dynein to KTs (Liang et al., 2007; Stehman et al., 2007; Vergnolle and Taylor, 2007) and the NE (Bolhy et al., 2011). Recent insights have revealed that the p150glued component of dynactin and Nde1/L1 compete for the same interaction domain on the DIC of the dynein complex, suggesting that dynein is either in complex with dynactin or with LIS1–Nde1/L1 (McKenney et al., 2011; Nyarko et al., 2012). Thus, it is possible that multiple distinct dynein complexes are formed with specialized functions. Although this is an attractive model, there is currently little in vivo evidence to support this model.

In addition to dynactin, LIS1, and Nde1/L1, numerous dynein-binding proteins have been identified to be important to target dynein to different subcellular structures. ZW10 (Starr et al., 1998; Whyte et al., 2008), hSpindly (Griffis et al., 2007; Gassmann et al., 2008, 2010), and CENPF (Vergnolle and Taylor, 2007) all contribute to the targeting of dynein–dynactin to KTs. Furthermore, dynein is recruited to the NE in G2/prophase in a BICD2-dependent manner (Splinter et al., 2010; Raaijmakers et al., 2012).

The complexity of the dynein complex itself, the large number of interaction partners, and its broad localization pattern suggest that its activity and localization are tightly controlled. However, it is largely unclear if and how different subunits and adaptors of the dynein complex contribute to distinct dynein functions. In addition, dynein localizes to many distinct sites in the cell, and it has proven very difficult to assign functions to specific dynein pools, which is key to obtain a mechanistic understanding of dynein's activity. Possibly, dynein forms different subcomplexes with its regulatory proteins, each performing a unique function, and this may have been overlooked, as commonly used approaches to perturb dynein activity in cells (e.g., antibody injections, expression of dominant-negative proteins) do not address the role of individual subunits. More recently, the use of siRNAs has evolved as a more specific way to study individual dynein subunits (Palmer et al., 2009). We use a similar siRNA-based screening approach to determine the contribution of each dynein subunit, dynactin subunit, and adaptor protein to the different functions of dynein in mitosis. Using this approach, we identified a set of dynein subunits, LIS1 and Nde1/L1, which are essential for all dynein functions in mitosis. Unexpectedly, we found that, although dynactin contributes to dynein recruitment to the NE and KTs, it is not required for dynein's function in organizing spindle microtubules. This surprising finding not only demonstrates that during cell division dynactin acts as a dynein targeting factor rather than a general activator, it also allows us to assign separate functions to distinct dynein pools.

Results

An RNAi-based screening approach to study dynein functions in mitosis

To get more insight into the regulation of dynein in mitosis and to the contribution of the individual subunits, we designed an siRNA library containing pools of four single siRNAs targeting each individual subunit of the dynein–dynactin complex and a number of dynein adaptor proteins. A complete overview of all the selected proteins, their accession numbers, gene ID, and protein size is listed in Table S1. Several dynein–dynactin subunits have multiple isoforms that could act functionally redundant (Pfister et al., 2006). Alternatively, the different isoforms might play roles in distinct processes and thereby contribute to dynein's specificity (Tai et al., 1999; Tynan et al., 2000). To reveal possible redundancies or functional differences between multiple isoforms, we included several combinations of siRNAs in our library.

As determined by qRT-PCR analysis, the knockdown efficiency of the individual siRNA pools ranged between 80–99%, 24 h after transfection (Fig. 1 A). The qRT-PCR analysis showed no detectable expression of DIC1 mRNA in our cell system,

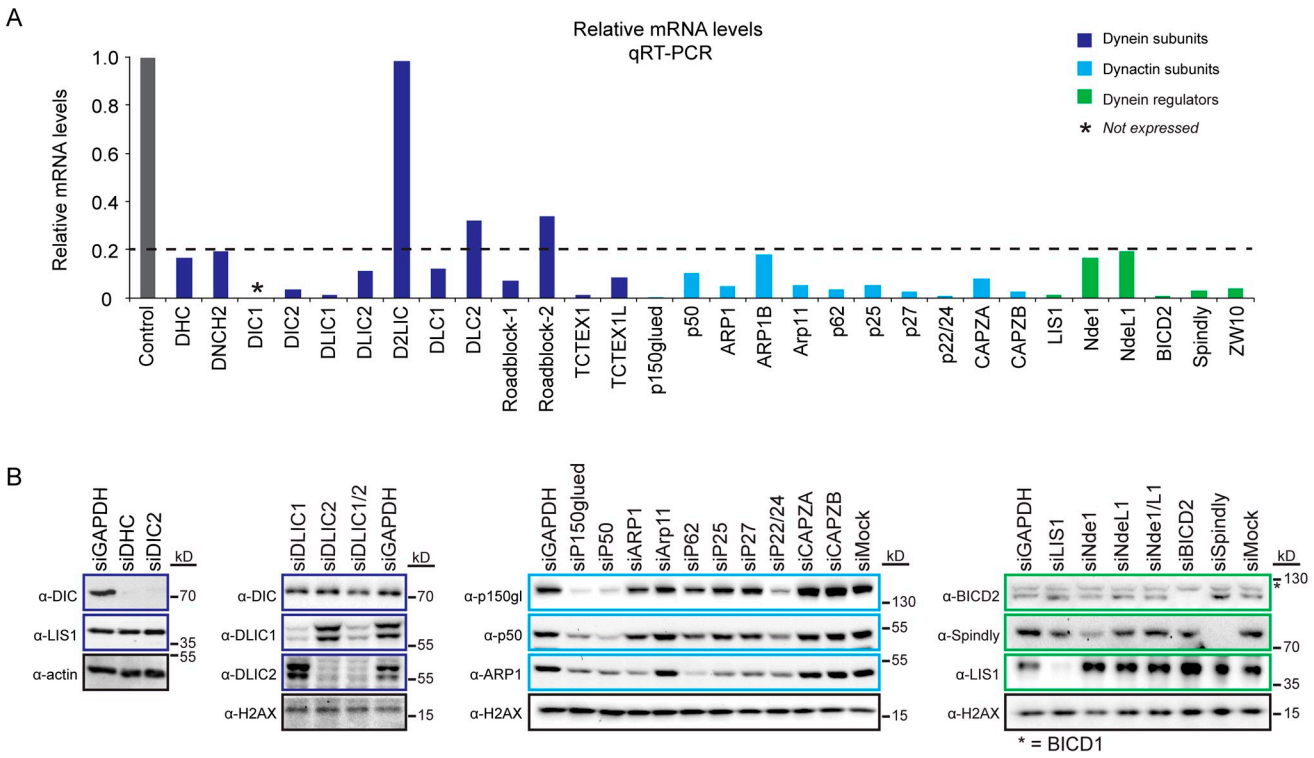

Figure 1. **Validation of siRNA library.** (A) Effects of siRNA pools on target gene down-regulation determined by qRT-PCR. cDNA was obtained from HeLa cells 24 h after transfection with siRNA pools targeting the indicated gene and mRNA levels were determined relative to the expression of this gene in control (siGAPDH) depleted cells. Levels are normalized against β-actin levels. Bars represent an average of a triplicate from a single experiment. (B) Western blot analysis to show effect of indicated siRNAs on total protein levels from mitotic HeLa cell lysates 72 h after transfection.

consistent with earlier reports that its expression is limited to neuronal tissue (Crackower et al., 1999). Therefore, we excluded DIC1 from further analysis. For the subset of proteins for which we could obtain working antibodies, we also tested knockdown efficiency 72 h after transfection on protein level and confirmed a substantial reduction in protein levels in all cases (Fig. 1 B). Notably, depletion of p150glued led to a decrease in p50 levels and vice versa. Similarly, depletion of p22/24 led to decreased levels of p150glued and to a lesser extent to decreased levels of p50. This indicates that depletion of either p150glued, p50, or p22/24, leads to destabilization of the projecting arm of the dynactin complex. Importantly, depletion of components from the projecting arm of dynactin also led to reduced levels of ARP1, indicating that loss of the projecting arm can affect the stability of the complete dynactin complex (Fig. 1 B; Jacquot et al., 2010). Finally, depletion of p62, p25, and p27, three components associated with the dynactin rod, led to decreased ARP1 levels, but did not affect the stability of p150glued or p50 (Fig. 1 B).

Anchoring of centrosomes to the NE in prophase

During late G2 and prophase, the centrosomes are positioned in close proximity to the nucleus in a dynein-dependent manner (Gönczy et al., 1999; Robinson et al., 1999; Splinter et al., 2010). Dynein exerts a pulling force on the centrosomes once it is recruited to the NE specifically in late G2. This G2-specific activation of dynein at the NE is thought to contribute to the separation of the centrosomes (Raaijmakers et al., 2012) and to the tearing of the nuclear envelope when cells enter mitosis (Salina et al., 2002). The dynein-dependent pulling forces are antagonized by kinesin-1 (Splinter et al., 2010). As a result, centrosomes are actively pushed away from the nucleus in late G2 when dynein is depleted. Indeed, in prophase cells depleted of DHC, centrosomes were displaced from the NE by an average distance of 18.84 µm (±1.72) (Fig. 2, A and B). Also depletion of DIC2 or Roadblock-1 led to a large increase in centrosome-nuclear distance in prophase. Depletion of DLIC1 and DLIC2 individually did not result in a severe phenotype, but combining the siRNAs directed against both DLIC1 and DLIC2 resulted in very pronounced centrosome mispositioning, similar to DHC depletion. Thus, although different functions have been assigned to DLIC1 and DLIC2 in a variety of processes (Tynan et al., 2000; Palmer et al., 2009), our results imply that during prophase, DLIC1 and DLIC2 act redundantly to position the centrosome close to the NE. Consistent with previously published results, we could confirm an essential function for dynactin in anchoring the centrosomes to the NE (Fig. 2, A and B; Splinter et al., 2010). Besides dynein–dynactin subunits, we also identified several adaptor proteins to be essential for the centrosome-anchoring function of dynein: depletion of LIS1 led to a severe centrosome detachment phenotype. Furthermore, co-depletion of Nde1 and NdeL1 resulted in a pronounced increase in centrosome–NE distance, whereas depletion of Nde1 or NdeL1 individually resulted in mild detachment or no phenotype at all, suggesting that, like DLIC1 and DLIC2,

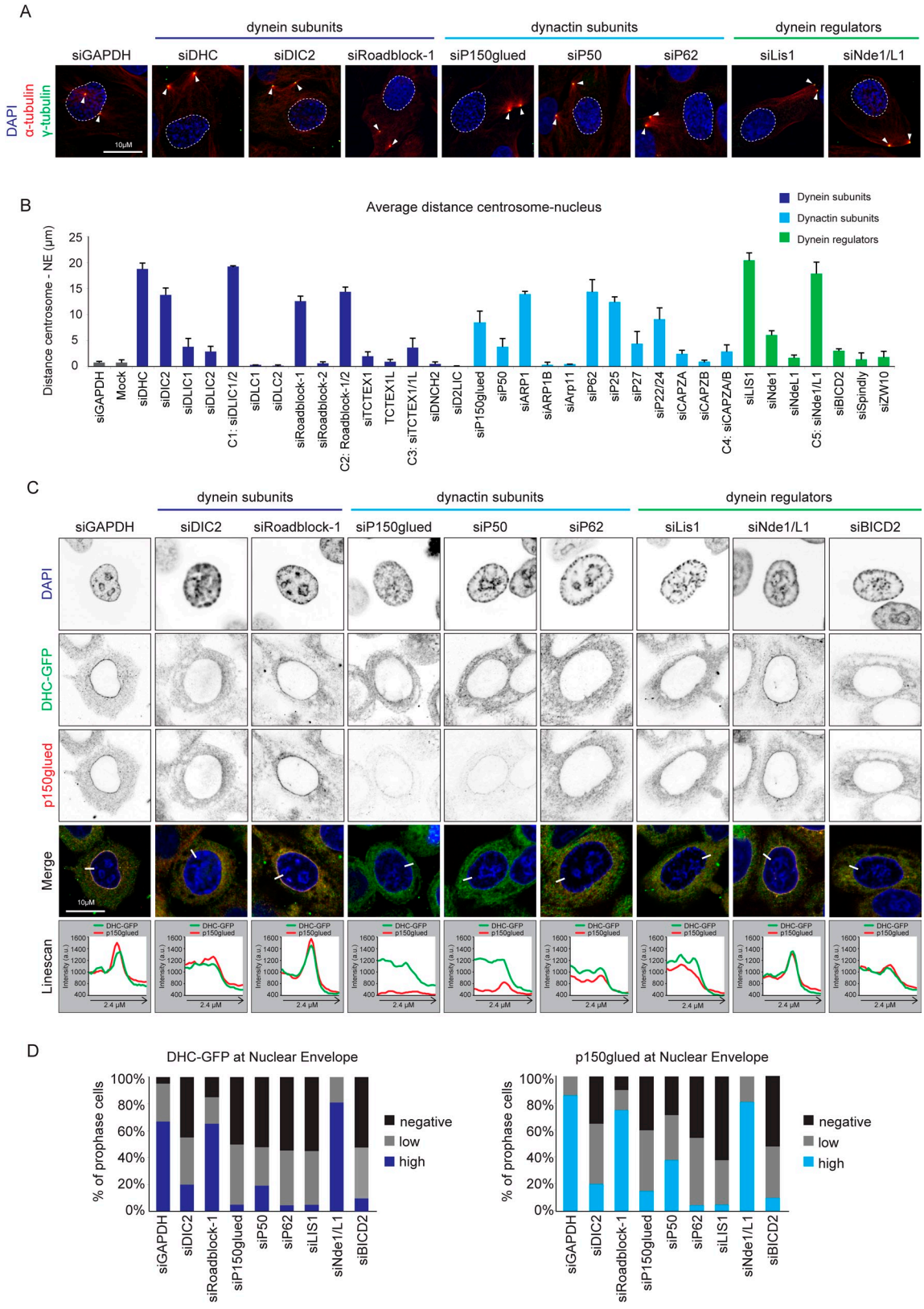

Figure 2. **Dynein-mediated centrosome anchoring to the NE requires dynactin, LIS1, and Nde1/L1.** (A) Representative images of centrosome detachment in prophase U2OS cells upon depletion of the indicated siRNAs. Centrosomes are stained with γ-tubulin, microtubules with α-tubulin, and the nucleus is visualized using DAPI. The dotted line indicates the outline of the nucleus. Arrows indicate the centrosomes. Bars, 10 μM. (B) Quantification of centrosome–nuclear distance in prophase cells 72 h after transfection with indicated siRNAs. Bars represent an average of three experiments (n = 20 centrosomes/experiment). Error bars represent SEM. (C) Representative images of nuclear envelope localization of DHC-GFP and p150glued after depletion of indicated siRNAs. Prophase cells were selected based on DNA condensation status. Line scans represent DHC-GFP (green line) and p150glued (red line) intensity at the NE. Bars, 10 μM. (D) Quantification of C (n > 20 cells/condition).

Nde1 and NdeL1 act redundantly in centrosome positioning. Finally, a minor defect in centrosome anchoring was observed upon BICD2 depletion. BICD2 was described previously to recruit dynein to the NE as well as the antagonizing kinesin-1 motor, which explains the moderate defect in centrosome detachment (Splinter et al., 2010; Bolhy et al., 2011). Similar results were obtained in HeLa cells for a subset of dynein–dynactin subunits and for LIS1 and Nde1/L1 (Fig. S2 A). Taken together, these results show that a large array of dynein and dynactin subunits, as well as multiple adaptor proteins, are required for dynein function at the NE.

To distinguish between activators and recruiters of the dynein motor complex, we tested multiple subunits that are essential for centrosome anchoring for their involvement in the targeting of dynein–dynactin to the NE in G2/prophase. To visualize dynein at the NE, we used HeLa cells expressing a BAC clone encoding mouse DHC with a GFP tag (Poser et al., 2008). We confirmed localization of both dynein and dynactin (p150glued) at the NE specifically during G2 (Fig. 2 C, first panel). We found that dynein and dynactin are interdependent for localization to the NE (Fig. 2 C; Splinter et al., 2012). Furthermore, we found that depletion of DHC, DIC2, p150glued, p50, p62, and LIS1 resulted in a clear reduction or loss of both DHC-GFP and p150glued from the NE in G2/prophase cells, similar to depletion of BICD2 (Fig. 2, C and D). Thus, the centrosome detachment in prophase that is observed upon depletion of these proteins can be explained by loss of dynein from the NE. In contrast, although depletion of Roadblock-1 or Nde1/L1 led to severe centrosome detachment in prophase (Fig. 2, A and B), we did not observe a decrease in the levels of either DHC-GFP or p150glued at the NE (Fig. 2, C and D). This suggests that Roadblock-1 and Nde1/L1 may be dynein activators rather than recruiters. It should be noted that we treated cells with nocodazole to be able to visualize dynein and dynactin localization to the NE, so we cannot exclude that Roadblock-1 and Nde1/L1 may be required for maximal accumulation of dynein–dynactin in the presence of microtubules.

Analysis of mitotic progression reveals distinct functions for dynein and dynactin

After nuclear envelope breakdown (NEB), dynein is essential for correct spindle formation (Verde et al., 1991; Vaisberg et al., 1993). Furthermore, dynein has been implicated in silencing the spindle assembly checkpoint (SAC) by transporting checkpoint proteins from attached KTs to the spindle poles (Howell et al., 2001; Wojcik et al., 2001). Using systematic depletion of all dynein–dynactin and adaptor proteins, combined with semi-automated microscopic analysis (Raaijmakers et al., 2009), we determined the effect of protein depletion on mitotic progression in both HeLa and U2OS cells (Fig. 3 A and Fig. S1 A). Depletion of DHC resulted in an increased mitotic index, with 24% mitotic cells compared with 5% in GAPDH-depleted HeLa cells. Depletion of several other dynein subunits, including DIC2, LIC1/2, and Roadblock-1 and a number of dynactin subunits, p50, ARP1, p62, and p22/24, as well as the adapter proteins LIS1, Nde1/L1, and Spindly also resulted in a significantly increased mitotic index ($P > 0.05$; Fig. 3 A). All subunits that resulted in a significantly higher mitotic index and resulted in an average mitotic index of at least two times standard deviation over siGAPDH upon depletion were selected for more detailed analysis. First, chromosome alignment defects were tested using HeLa cells arrested in mitosis using the proteasome inhibitor MG132. Strikingly, the increased mitotic index observed after interference with dynactin function is most likely not due to major problems in chromosome alignment as are observed after depletion of dynein subunits (Fig. 3, B and C). Live-cell imaging of HeLa cells stably expressing H2B-YFP revealed that the mitotic delay after depletion of different dynein subunits coincides with a gross defect in chromosome alignment (Fig. 3, D and E), whereas depletion of all the dynactin subunits we tested (p50, p62, p22/24, or ARP1) did not result in chromosome alignment defects (Fig. 3, D and E). Instead, dynactin-depleted cells spend long periods of time in metaphase, without obvious loss of chromosomes from the metaphase plate (although in cells delayed >350 min, chromosomes eventually start to scatter, consistent with progressive loss of chromosome cohesion during a prolonged mitosis; see Fig. S1 B; Daum et al., 2011; Stevens et al., 2011). In line with the metaphase delay observed in the dynactin-depleted cells, we also observed long periods of mitotic delay with aligned chromosomes in the few cells depleted of different dynein subunits that do manage to align their chromosomes (Fig. 3 D). In contrast to depletion of dynactin subunits, depletion of LIS1 and Nde1/L1 led to a dramatic defect in chromosome alignment (Fig. 3, D and E). Finally, in line with previous findings (Griffis et al., 2007; Gassmann et al., 2010), we observed an increase in mitotic index after depletion of Spindly, characterized by a large increase in misalignments (Fig. 3, A–E).

Dynactin is dispensable for correct MT–KT attachments

Although chromosome alignment is readily established in the dynactin-depleted cells, this does not exclude that the fidelity of the MT–KT attachments is perturbed, resulting in the prolonged "metaphase-like" arrest. Therefore, we set out to determine the quality of the KT–MT attachments in more detail. First, we studied the presence of cold-stable MTs in dynactin-depleted cells as a read-out for the amount of stable K-fibers. Dynactin-depleted cells showed no reduction in the amount of cold-stable MTs compared with GAPDH-depleted cells (Fig. 4, A and B). Hec1, a well-established regulator of KT–MT attachments, was used as a positive control (Fig. 4, A and B). Next, we studied the presence of Astrin on KTs, which only localizes to KTs that are under tension (Schmidt et al., 2010). Indeed, nocodazole-treated cells display very low levels of Astrin, whereas GAPDH-depleted control cells showed high Astrin levels on all KTs (Fig. 4 C). Although DHC-depleted cells showed decreased Astrin localization to a subset of KTs, dynactin-depleted cells displayed high Astrin levels, indicating that all KT pairs are under tension (Fig. 4 C). In line with these results, we measured no decrease in inter-KT tension upon depletion of different

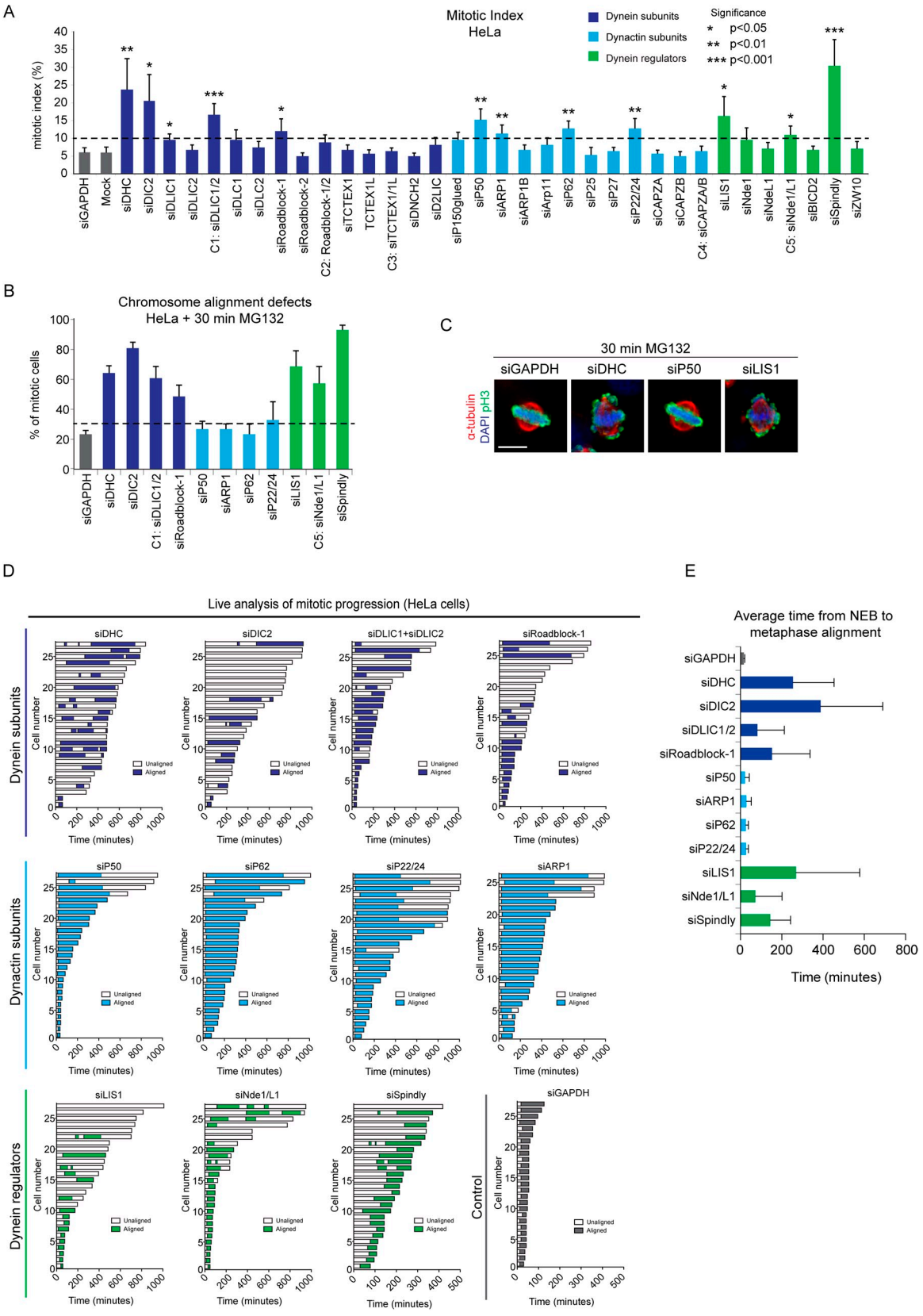

Figure 3. **Analysis of mitotic progression reveals different functions for dynein and dynactin.** (A) HeLa cells were transfected with the siRNA library and mitotic index was determined 72 h after transfection, as described in the Materials and methods section. The dotted line indicates the siGAPDH average + 2× standard deviation. Bars represent an average of four individual experiments and error bars display SEM. Student's *t* test was performed to determine statistical significance. (B) HeLa cells were transfected with indicated siRNAs. Cells were fixed 72 h after transfection and stained with α-tubulin to visualize the microtubules, phospho-Histone 3 (pH3) to detect mitotic cells, and DAPI to visualize the DNA. Bars represent the percentage of mitotic cells displaying

dynactin subunits (Fig. 4 D). As a final assay to test the fidelity of the MT–KT attachments, we filmed HeLa cells stably expressing H2B-YFP transfected with GAPDH siRNA, ARP1 siRNA, DHC siRNA, or a low dose of Taxol (1 nM) as a positive control. After 180 min, cells were forced into anaphase by addition of the Mps1 inhibitor Mps1-IN-1 (Kwiatkowski et al., 2010) and the amount of missegregating chromosomes in anaphase was scored (Fig. 4, E and F). Forcing cells treated with a low dose of taxol or transfected with DHC siRNA into anaphase resulted in an increase in the amount of missegregating chromosomes, indicating that not all KTs were properly bi-oriented. In striking contrast, ARP1-depleted cells showed no increase in missegregating chromosomes. Although we cannot exclude that there are minor errors in KT–MT attachment in the ARP1-depleted cells, this result indicates that all KTs are bi-oriented properly in the mitotic arrest induced by the inhibition of dynactin, indicative of a true metaphase arrest. Furthermore, all ARP1- and DHC-depleted cells rapidly proceeded to anaphase upon Mps1 inhibition, indicating that the mitotic arrest is checkpoint dependent in both cases.

Dynein has previously been implicated in silencing the mitotic checkpoint by stripping checkpoint proteins from kinetochores (Howell et al., 2001; Wojcik et al., 2001). To test whether a failure of stripping checkpoint proteins of the KTs is the cause of the observed metaphase arrest in dynactin-depleted cells, we stained for several checkpoint proteins (Fig. S3, A–D). We synchronized cells by releasing them from RO-3306, a potent CDK1 inhibitor (Vassilev et al., 2006), and we used nocodazole-treated cells as a control. Surprisingly, we could not observe BubR1, MAD1, CDC20, or Spindly at the KTs of ARP1-depleted cells. On the contrary, although most KTs in DHC-depleted cells are negative for the tested checkpoint proteins, some KTs displayed detectable levels (Fig. S3, A–D, insets). Thus, we find no obvious stripping defect of checkpoint proteins at KTs, but the arrest is due to persistent checkpoint signaling.

We next studied dynein recruitment to KTs (Fig. 5, A and B). Using HeLa cells stably expressing DHC-GFP, we could confirm the involvement of Spindly and ZW10 in the recruitment of dynein to KTs (Starr et al., 1998; Griffis et al., 2007; Gassmann et al., 2008; Whyte et al., 2008). Although we do observe a small reduction in dynein levels, we could not confirm a significant role for Nde1 in dynein recruitment to the KT, whereas we do find a small but significant reduction upon depletion of NdeL1 (Vergnolle and Taylor, 2007). We find that ∼80% of dynein retains at the KTs in Nde1/L1 depletions, suggesting that other pathways act redundant with Nde1/L1 in dynein recruitment. Furthermore, in contrast to previous studies, interfering with LIS1 resulted in severely reduced dynein at the KT (Fig. 5, A and B; Faulkner et al., 2000; Tai et al., 2002). In addition, we found that DIC2, Roadblock-1, and TCTEX1/1L all contribute to recruitment of the dynein complex to the KT as well as the dynactin subunits p150glued, p50, ARP1, p62, p25, and p22/24. We found similar results in prometaphase cells not treated with nocodazole (Fig. S4). It should be noted that we find a small pool of dynein retained at KTs when dynactin is depleted (Fig. 5 B). Arguably, this residual dynein pool promotes chromosome alignment in the dynactin-depleted cells. However, depletion of different dynein subunits, under which DIC2 and DLIC1/2 results in a similar or even less prominent displacement of dynein from the KT, but unlike dynactin-depletion, these cells have major chromosome congression defects (Fig. 3, B–E; Fig. 5). Taken together, these results suggest that the function of dynein in chromosome alignment does not depend on its presence at kinetochores. Moreover, these data suggest that the major role of KT–dynein is to silence the SAC.

Dynactin is dispensable for dynein-dependent force generation in the mitotic spindle

A key player in bipolar spindle assembly is the plus end–directed motor Eg5 (kinesin-5). Eg5 forms homotetramers, allowing it to slide anti-parallel microtubules apart (Kashina et al., 1996; Kapitein et al., 2005). Without Eg5 activity, human cells fail to separate their centrosomes and form a monopolar spindle (Sawin et al., 1992; Blangy et al., 1995; Kashina et al., 1996). Previous studies from our laboratory and others have demonstrated that dynein can antagonize the outward force in the spindle generated by Eg5, as inhibition of dynein function rescues spindle bipolarity in Eg5-inhibited cells (Mitchison et al., 2005; Tanenbaum et al., 2008; Ferenz et al., 2009). To identify the components essential for the dynein-mediated force generation in the spindle, we used our siRNA collection to screen for a rescue of spindle bipolarity in Eg5-inhibited cells. The majority of HeLa cells treated with the small molecule Eg5 inhibitor STLC (DeBonis et al., 2004) form a monopolar spindle. However, when DHC is depleted (Fig. 6 A; Fig. S2 B), a large fraction of cells form a bipolar spindle, consistent with our previously published work (Tanenbaum et al., 2008). Also depletion of the dynein subunits DIC2, Roadblock-1, and DLIC1/DLIC2 led to a prominent rescue of spindle bipolarity in STLC-treated cells. Interestingly, these are the same subunits that are essential for mitotic progression and centrosome anchoring to the NE (Fig. 3 A; Fig. 2 B), suggesting that, at least for these functions, there is no specificity

chromosomes that are not aligned on the metaphase plate. *n* = 3 experiments (50 cells/experiments) and error bars represent SEM. (C) Representative images of cells quantified in B. Bar, 10 µM. (D) Quantification of mitotic timing and chromosome alignment of HeLa cells stably expressing YFP-H2B. Cells were transfected with indicated siRNAs and blocked in thymidine 48 h after transfection. After 16 h, cells were released from the thymidine block. Live-cell imaging started 6 h after the release for the duration of 18 h. Because of the effect of the siRNA on cell survival, cells depleted for Spindly were imaged 48 h after transfection. Images were acquired every 6 min. Bars in the graph represent total time spent in mitosis for individual cells from a single experiment. White bars indicate time spent with unaligned chromosomes and colored bars indicate time spent with full chromosome alignment. Starting point is NEB and end of the bar represents either anaphase or cell death in mitosis. (E) Average time from NEB to full chromosome alignment from the cells in C. Error bars represent SD.

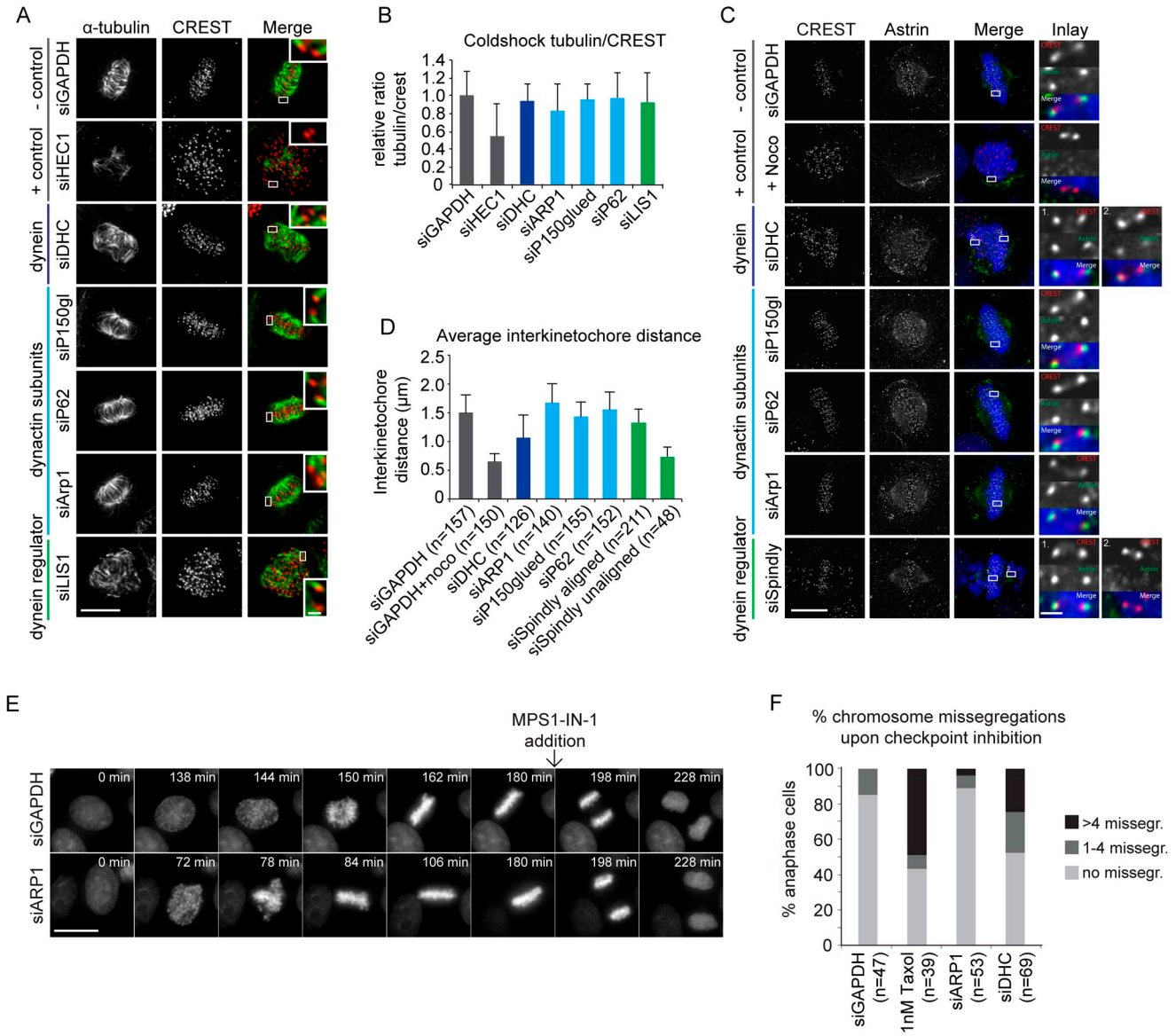

Figure 4. **Dynactin is dispensable for correct MT–KT attachments.** (A) Analysis of cold-stable microtubules. HeLa cells were transfected with indicated siRNAs for 72 h. Cells were treated with cold medium (4°C) for 20 min before fixation. Cells were subsequently fixed and stained for α-tubulin and CREST. Images are maximum projections of deconvolved z-stacks. Bar, 10 µm. Insets are magnified views of single kinetochore pairs selected from a single z-slice. Bars (insets), 1 µm. (B) The average α-tubulin signal was quantified and normalized against CREST after background correction (n = 10 cells per condition). (C) Analysis of Astrin localization at KTs. HeLa cells were transfected with indicated siRNAs for 72 h. Nocodazole-treated cells were used as a positive control. Cells were fixed and stained for CREST and Astrin. Insets are enlargements of individual KT pairs. Bar, 10 µm (insets, 1 µm). (D) Inter-KT distance. HeLa cells were transfected with indicated siRNAs and treated with MG132 for 1 h before fixation. After fixation, cells were stained with CREST antibody. The distance between CREST signals was measured. (E) HeLa cells stably expressing YFP-H2B were transfected with siRNA against GAPDH or against ARP1. Cells were imaged every 6 min. After 180 min, cells were forced into anaphase by inhibiting the mitotic checkpoint by addition of 1 µM of the Mps1 inhibitor Mps1-IN-1. Two representative examples are shown. Bar, 10 µm. (F) Cells were transfected with indicated siRNAs. The amount of missegregating chromosomes in anaphase was scored for the indicated amount of cells per condition.

between the different dynein subunits themselves. The STLC-induced monopolar spindles could also be rescued by depletion of LIS1 or Nde1/NdeL1. Strikingly, we did not observe a rescue of spindle bipolarity upon depletion of any dynactin subunit (Fig. 6 A; Fig. S2 B), demonstrating that dynactin is not essential for dynein-mediated force generation in the spindle. Thus, consistent with the results on chromosome alignment, a complex of dynein together with LIS1 and Nde1/L1 controls force generation in the spindle, independent of dynactin.

To resolve if the force-generating function of dynein in the spindle affects spindle elongation, we studied the average spindle length in HeLa cells. In line with the results obtained in the Eg5 antagonism assay, we found that depletion of DHC, DIC2, or Roadblock-1 led to a small but significant increase in average spindle length (Fig. 6 B). Depletion of LIS1 or Nde1/L1 also led to a small increase. However, no defects in spindle length were observed after depletion of different dynactin subunits. These results are consistent with a role for

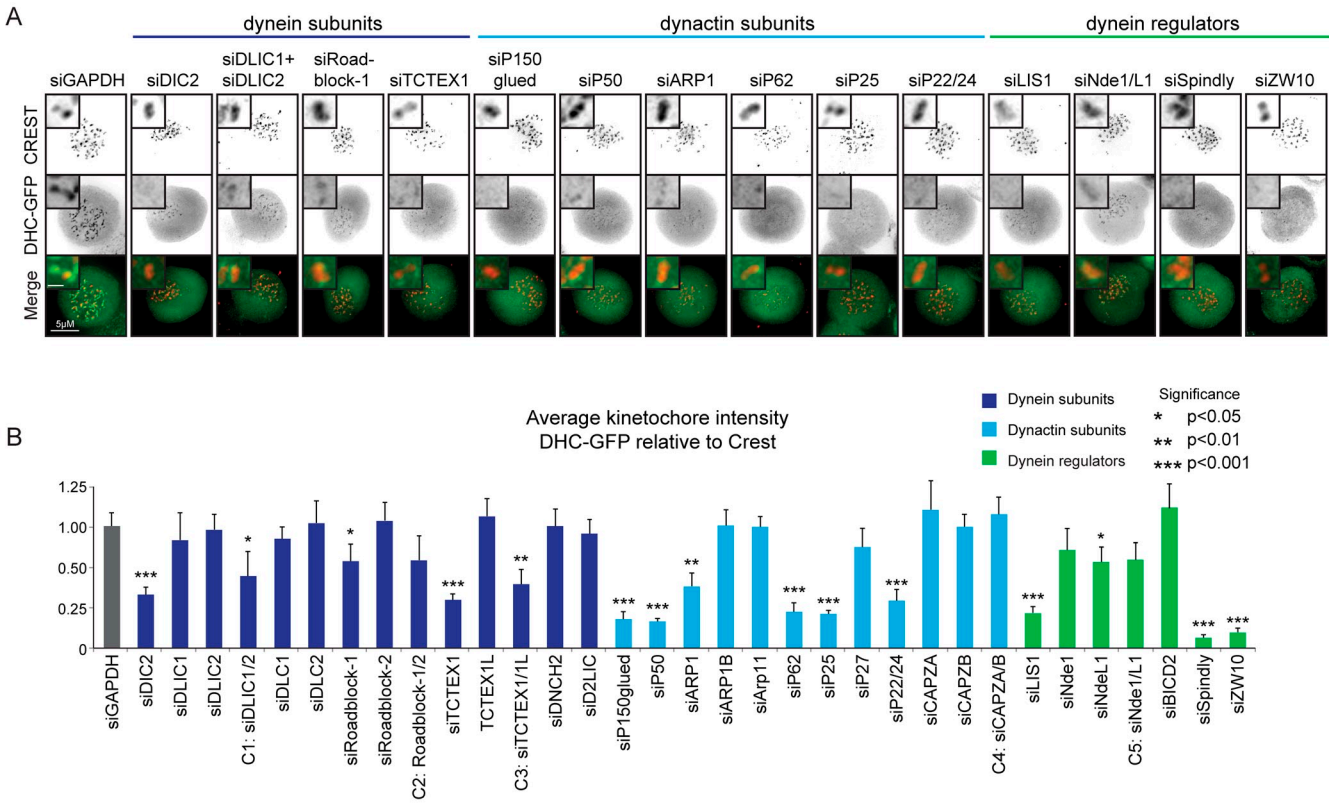

Figure 5. **Dynein recruitment to kinetochores.** (A) DHC-GFP–expressing HeLa cells were transfected with indicated siRNAs. 48 h after transfection, cells were treated with nocodazole overnight. Cells were fixed and stained with anti-GFP antibody and a CREST antibody to visualize centromeres. Bar, 5 μm (insets, 0.5 μm). (B) The relative level of DHC at the KTs was determined from maximum projections for all KT pairs (>50 KTs/cell) in a cell for >5 cells/condition and corrected for cytoplasmic levels. Student's *t* test was performed to determine statistical significance.

dynein, LIS1, and Nde1/L1 in inward force generation in the mitotic spindle and show that dynactin is dispensable for this function.

Dynein-dependent focusing of spindle poles does not depend on dynactin

The ability of dynein to focus microtubules in the pole region of the spindle is an important aspect of dynein function in spindle organization (Heald et al., 1996; Goshima et al., 2005). Consistent with these studies, depleting DHC in U2OS or HeLa cells results in spindles with large arrays of unfocused microtubules and/or spindles that lose the attachments to their centrosomes (Fig. 7 A). We next tested a subset of dynein–dynactin components and adaptor proteins for their involvement in spindle microtubule organization and found that depletion of three different dynein subunits results in severe spindle pole focusing defects (Fig. 7 B; Fig. S2 C). Similar defects were observed after depletion of LIS1 or Nde1/NdeL1. Strikingly, although the amount of DHC-GFP at the spindle poles is slightly reduced in dynactin-depleted cells (Fig. S5), no defects in pole focusing were observed after depletion of three different dynactin subunits (Fig. 7 B; Fig. S2 C). This suggests that also for dynein-dependent microtubule focusing, dynactin is completely dispensable. Thus, similar to results described above, dynein acts together with LIS1 and Nde1/L1, but independently of dynactin to control spindle organization.

Discussion

Components of the dynein motor essential for dynein function in mitosis

The dynein complex itself contains a variety of subunits. The DHC is essential for the stability of the complete complex and depletion of the DHC is therefore expected to result in loss of all dynein functions. Indeed, DHC RNAi produced a phenotype in all of the assays we used to study dynein functions. In addition, we found that depletion of the DIC2, which is not essential for complex stability (Palmer et al., 2009), is also essential for all mitotic functions of dynein tested here (see Figs. 2, 3, 6, and 7). The DIC is a major binding platform for multiple dynein adaptor proteins including Nde1/L1 and dynactin, which explains its central role in dynein function. Besides DIC2, we found that the dynein LICs are essential for all dynein functions in mitosis. Interestingly, DLIC1 and DLIC2 act almost completely redundant because depletion of the individual DLICs resulted in minor mitotic defects, but combining siRNAs targeting both DLIC1 and DLIC2 led to severe phenotypes, comparable to depletion of the DHC. Furthermore, we found that the Roadblock-1 light chain is required for all dynein functions studied here. Roadblock-1 forms a homodimer that can bind directly to the intermediate chains of the dynein complex (Susalka et al., 2002; Hall et al., 2010). Despite the extensive knowledge acquired on the structure and binding of Roadblock-1

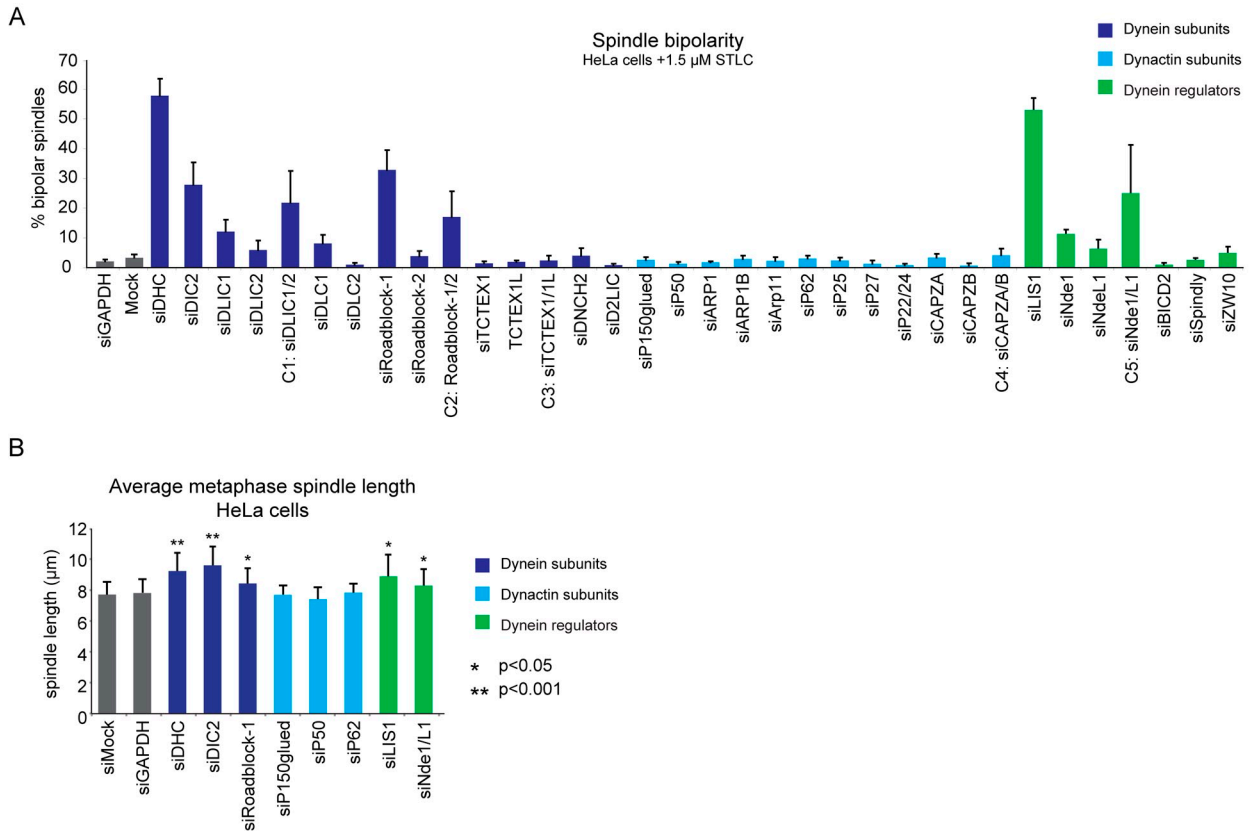

Figure 6. **Dynactin is dispensable for dynein-dependent force generation in the mitotic spindle.** (A) Quantification of the percentage of bipolar spindles in HeLa cells treated with 1.5 µM STLC. Remaining spindles are all monopolar. Bars are an average of three independent experiments (n = 50 cells/experiment). Error bars represent SEM. (B) Average mitotic spindle length. Cells were transfected with indicated siRNAs. 72 h after transfection, cells were fixed and stained with α-tubulin to visualize the mitotic spindle. The length of the spindle was determined for >20 cells/condition in two independent experiments. Error bars represents SD.

(Susalka et al., 2002; Song et al., 2005; Hall et al., 2010), the contribution of Roadblock-1 to dynein function in mitosis has remained elusive. Because we find that Roadblock-1 depletion leads to a complete loss of dynein function in mitosis, without affecting its localization (in case of the NE; Fig. 2, B–D), we suggest that this light chain is an essential component of the dynein motor complex required for its full activity in vivo.

Depletion of LIS1 results in mitotic defects that are very similar to defects observed after depletion of DHC, DIC, DLIC, or Roadblock-1. LIS1 was previously shown to promote dynein-mediated force generation in vitro (McKenney et al., 2010; Huang et al., 2012). We find that binding to the regulatory proteins LIS1 and Nde1/NdeL1 is essential for most mitotic dynein functions, but that LIS1 also plays critical roles in targeting the dynein complex to different subcellular structures in mitosis. In contrast, Nde1/L1 is not required for localization of dynein to the majority of sites, but is critical for all dynein functions tested. In vitro data has suggested that the presence of Nde1/L1 might enhance the effects that LIS1 executes on dynein activity (McKenney et al., 2010; Huang et al., 2012). In line with this, we find that the presence of Nde1/L1 is important for all dynein-dependent functions tested here, which are all processes that require a high load-bearing state of the dynein complex.

Dynactin-independent functions of dynein

The interaction of dynein with the multi-subunit dynactin complex has been thought to be critical for most, if not all, dynein functions. In this study we find that both components from the arm (p150glued, p50, and p22/24) and from the rod (ARP1 and p62) are critical for all dynactin-dependent functions tested here. Depletion of p25 results in reduced ARP1 levels (Fig. 1 B). In line with this, we also observe defects when p25 is depleted in most assays. Although depletion of p27 also leads to decreased ARP1 levels, albeit a bit less compared with p25 depletion, we observe only minor defects upon p27 depletion. It seems most likely that the amount of protein depletion might be critical for loss of dynactin function and that we are simply not sufficiently reducing p27 protein levels to observe major defects in our assays. Unfortunately, we have no antibodies to test this possibility. Finally, depletion of the capping proteins CAPZA and CAPZB does not result in any major mitotic phenotype, suggesting that these proteins are not critical for dynactin function in mitosis.

Although we find that the dynactin complex contributes to the targeting of dynein to the NE and KTs, we find that dynactin is completely dispensable for dynein-mediated MT organization within the spindle. This unexpected discrimination in dynactin dependency allows assignment of specific functions of

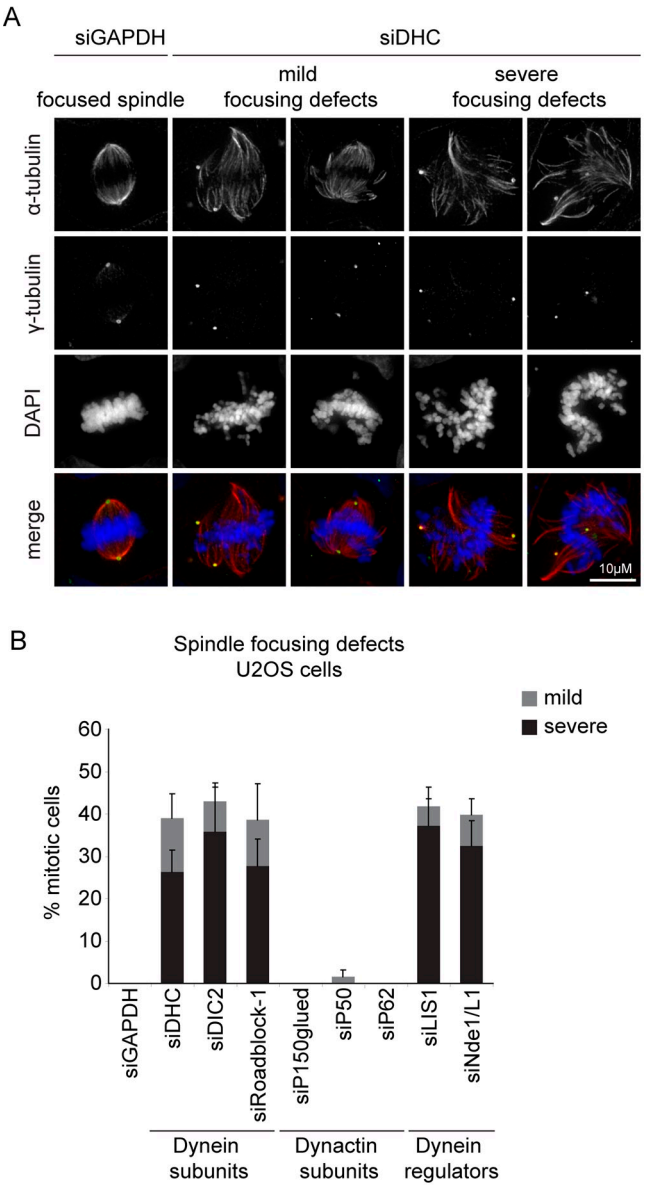

Figure 7. **Dynein-mediated spindle pole focusing does not depend on dynactin.** (A) Immunofluorescent images of spindle pole focusing defects upon DHC depletion. Cells were stained with α-tubulin to visualize microtubules; γ-tubulin to visualize the centrosomes, and the DNA was stained with DAPI. Bar, 10 μM. (B) Quantification of spindle pole focusing defects in U2OS cells 72 h after transfection with indicated siRNAs. $n = 75$ cells/condition in three independent experiments. Error bars represent SD.

dynein to separate motor complexes of distinct composition, providing important mechanistic insights into dynein's numerous functions. The finding that perturbation of alignment, spindle pole focusing, and force generation in the spindle do not correlate with the displacement of dynein from KTs (compare p50 to DIC2 depletion; Fig. 5; Fig. 3, B–E; Fig. 6; and Fig. 7) suggest that KT–dynein is not involved in these processes. If so, then this would also imply that the gross defects in chromosome alignment observed after dynein depletion are indirectly due to defects in spindle microtubule organization and should not be taken as evidence for a role for the KT-associated pool of dynein in chromosome congression. However, we cannot exclude that the residual KT–dynein pool contributes to chromosome congression in the dynactin-depleted cells.

Although our data indicate that dynactin is not required for spindle formation, a role for dynactin in spindle organization was previously suggested based on experiments in *Xenopus* extracts (Wittmann and Hyman, 1999; Mitchison et al., 2005) and COS-7 cells (Echeverri et al., 1996). However, these conclusions were based on experiments in which excess p50/dynamitin was necessary to generate the spindle defects, levels that are 10-fold higher than the levels needed for biochemical interruption of the dynactin complex (Wittmann and Hyman, 1999). In this respect it is of interest to note that excess p50 causes disruption of the dynactin complex, leading to enhanced levels of free p150glued (Wittmann and Hyman, 1999). This means that the commonly applied method of overexpression of p50 to block dynactin function is clearly distinct from depletion of p50 because overexpression of p50 leads to release of the p150glued subunit but not to its degradation (Eckley et al., 1999; Melkonian et al., 2007; Jacquot et al., 2010). Because p150glued can bind to dynein directly, the release of p150glued from the dynactin complex could prevent other proteins to bind to the same domain on the DIC, such as Nde1/L1 (McKenney et al., 2011), necessary for high load-bearing dynein activity. We and others demonstrate that depletion of p50 results in decreased p150glued levels (Fig. 1 B; Jacquot et al., 2010), preventing such possible dominant-negative effects. This not only provides an explanation for the different conclusions drawn on dynactin's involvement in spindle organization between different studies, but it also demonstrates how different inhibition methods (i.e., protein overexpression versus protein depletion) can result in different outcomes.

Dynactin-dependent functions of dynein

Depletion of dynactin leads to a prominent delay in metaphase without obvious defects in spindle organization or chromosome congression (Fig. 4). We find that the mitotic delay is checkpoint dependent, as inhibition of Mps1 resulted in rapid exit from mitosis in both dynein- and dynactin-depleted cells (Fig. 4 E; unpublished data). Importantly, chromosome segregation was completely normal, supporting the notion that all KTs were properly bi-oriented and the defect is in SAC silencing. Although a role for dynein has previously been described in checkpoint silencing by stripping checkpoint proteins from correctly attached MTs (Howell et al., 2001; Wojcik et al., 2001), we do not observe residual checkpoint proteins at the KTs of ARP1-depleted cells upon bi-orientation (Fig. S3). As dynactin acts as an anchor for dynein at the KT (Fig. 5), we use dynactin depletion as a tool to study the role of KT–dynein in the silencing of the mitotic checkpoint without perturbing KT–MT attachments. The mechanism by which the checkpoint proteins are removed from the KTs in dynactin-depleted cells remains unclear and we cannot exclude that this is executed by a residual dynein pool at the KT that is recruited via a dynactin-independent pathway (ZW10, Nde1/NdeL1). Alternatively, there might still be a stripping defect, but the levels of the different checkpoint proteins could be below the detection limit in our assays. Finally, dynein–dynactin might play a role in the $p31^{comet}$ pathway, as depletion

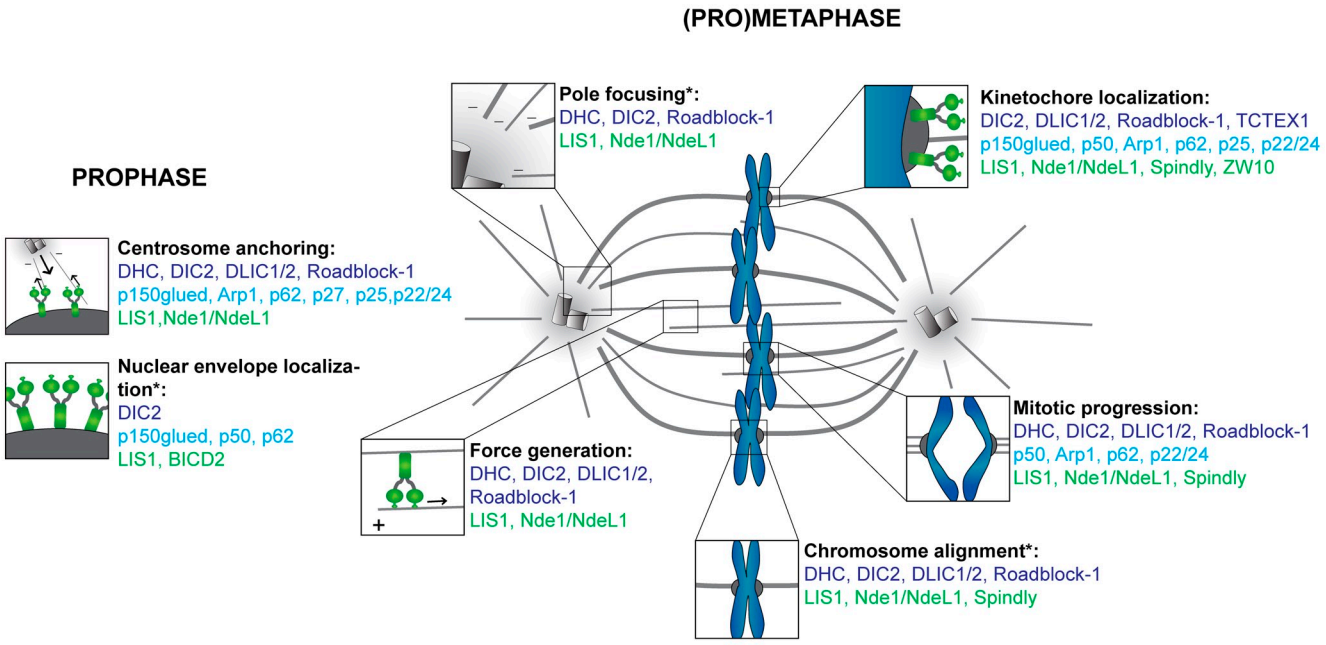

Figure 8. **Summary of results.** Overview of results obtained in this study. The asterisks indicate phenotypes that were only studied for a subset of the siRNA library. Dynein subunits are indicated in dark blue, dynactin subunits in light blue, and the adaptor proteins in green.

of this checkpoint antagonist leads to a very similar metaphase delay with mature KT–MT attachments without sustained checkpoint signaling from the KTs (Hagan et al., 2011). Taken together, our data provide further support for a role of dynein–dynactin in checkpoint silencing. However, more work is required to resolve the underlying mechanism, which may or may not act through kinetochore stripping.

Microtubule organization requires a high load-bearing state of dynein

Our results favor a model in which dynein needs to be in complex with LIS1 and Nde1/L1 to execute its functions in spindle organization. Binding to LIS1 and Nde1/L1 generates a motor complex with high load-bearing activity (McKenney et al., 2010; Huang et al., 2012), implying that prominent dynein-dependent forces are required to organize the mitotic spindle. This is not entirely unexpected because dynein needs to antagonize significant outward forces produced by other motor proteins, such as Eg5 and Kif15 (Sawin et al., 1992; Kashina et al., 1996; Tanenbaum et al., 2009; Vanneste et al., 2009). Our data show that dynactin is not required for this, although we do find that dynactin plays an important role in targeting dynein to various subcellular structures in mitosis. These data imply that during mitosis, rather than acting as a processivity factor, dynactin acts to recruit dynein to selected sites to perform a particular function. Together, our data suggest that the role that dynein plays in spindle organization does not depend on selective recruitment by dynactin, but instead demands dynein to produce sufficient power to antagonize the forces produced by other motors and the highly dynamic microtubules.

In summary, we have been able to resolve the contribution of the individual dynein subunits, the dynactin complex, and several dynein adaptor proteins to the numerous functions of the dynein motor complex in mitosis. Our data reveal which subunits are essential for dynein function in mitosis. In addition, our data show which of the single recruiters and/or activators are required for a specific dynein function in mitosis (for a summary see Fig. 8). This makes it possible to selectively interfere with a particular function of dynein in mitosis, and will be of great benefit for future studies to resolve how the distinct mitotic functions of dynein are differentially regulated.

Materials and methods

Cell culture, transfection, and drug treatment

U2OS and HeLa cells were cultured in DMEM (Gibco) with 6% FCS, 100 U/ml penicillin, and 100 µg/ml streptomycin. siRNA (OTP pools; Thermo Fisher Scientific) were transfected using reverse transfection with Hiperfect (QIAGEN) according to the manufacturer's guidelines. STLC and nocodazole were dissolved in DMSO and used with a final concentration of 1.5 µM and 250 ng/ml, respectively.

Immunofluorescence

Cells were grown on 10-mm glass coverslips and fixed in 3.7% formaldehyde/0.5% Triton X-100 in PBS for 20 min. All primary antibodies were incubated at 4°C overnight and secondary antibodies were incubated for 2 h at room temperature. The following antibodies were used: anti–α-tubulin (1:10,000; Sigma-Aldrich), anti–γ-tubulin (1:500; Sigma-Aldrich), anti-CREST (1:1,000; Cortex Biochem), anti-pH3 (1:1,000; EMD Millipore), and anti-GFP (1:5,000; custom made). Secondary antibodies for immunofluorescence were Alexa Fluor 488, Alexa Fluor 568, and Alexa Fluor 647 (Molecular Probes). DAPI was added to all samples before mounting using Vectashield mounting fluid (Vector Laboratories). Confocal images were acquired on a microscope (LSM 510 META; Carl Zeiss) with a Plan Apochromat 63×/NA 1.4 objective with 1-µm z-stacks. Images in Fig. 4 (A and C) and Fig. 5 A were acquired on a microscope (Deltavision Elite; Applied Precision), taking 200-nm z-stacks using a PlanApo N 60×/NA 1.42 objective (Olympus) and a camera (Coolsnap HQ2; Photometrics). Images were analyzed after deconvolution using SoftWoRx (Applied Precision). Figures were generated by maximum intensity projection of entire cells using Softworx and ImageJ (National Institutes of Health). Brightness and contrast were adjusted with Photoshop 6.0 (Adobe). Mitotic indexes were determined using automated image acquisitioning. Cells were grown in 96-well plates (Viewplate-96;

PerkinElmer) in 100 µl of culture medium. Cells were fixed by addition of 50 µl of an 11% formaldehyde/1.5% Triton X-100 solution for 15 min to prevent loss of mitotic cells. Cells were then washed with PBS and stained with anti-pH3 antibody and DAPI. Image acquisition was performed using a Cellomics ArrayScan VTI Reader (Thermo Fisher Scientific) using a 10×/NA 0.50 objective and five images were acquired per well, which contained around 1,000–2,000 cells in total. Image analysis was performed using a Cellomics ArrayScan HCS Reader (Thermo Fisher Scientific). Cells were identified on the basis of DAPI staining and they were scored as mitotic if the pH3 staining reached a preset threshold. All images and automated image quantifications were visually checked.

Time-lapse microscopy

HeLa cells stably expressing YFP-H2B were reverse transfected with siRNA and plated in a 96-well plate (BD). Images were obtained on a confocal system (model SP5; Leica), in a permanently heated chamber in Leibovitz L15 CO_2-independent medium. Images were acquired every 6 min using a Plan Apo 20×/NA 0.70 objective (Leica). Z-stacks were acquired with 2-µm intervals. Images were processed using ImageJ software.

RNA isolation and qRT-PCR analysis

For RNA preparations, HeLa cells were seeded in 96-well plates and transfected as described above. Cells were harvested 24 h after transfection by trypsinization. Total RNA was extracted from the cells using the InviTrap RNA Cell HTS 96 kit and quantified using NanoDrop (Thermo Fisher Scientific). cDNA was synthesized using SuperScript III reverse transcription, random primers (Promega), and 100 ng of total RNA according to the manufacturer's protocol. Primers were designed with a melting temperature close to 60 degrees to generate 90–120-bp amplicons, mostly spanning introns (see Table S2 for primer sequences). cDNA was amplified for 40 cycles on a cycler (model CFX96; Bio-Rad Laboratories) using SYBR Green PCR Master Mix (Applied Biosystems). Target cDNA levels were analyzed by the comparative cycle (Ct) method and values were normalized against β-actin expression levels.

Western blotting

Cells were transfected with indicated siRNAs. After 72 h, cells were harvested and lysed using Laemmli buffer (120 mM Tris, pH 6.8, 4% SDS, and 20% glycerol). Equal amounts of protein were separated on a polyacrylamide gel and subsequently transferred to nitrocellulose membranes. Membranes were probed with the following primary antibodies: anti-dynein intermediate chain (70.1, 1:1,000; Sigma-Aldrich), anti-LIS1 (1:2,000; a gift from O. Reiner, Weizmann Institute of Science, Rehovot, Israel), anti-p150glued (1:1,000; Transduction Laboratories), anti-p50 (1:1,000; BD), anti-actin (1:1,500; Santa Cruz Biotechnology, Inc.), anti-DLIC1 and anti-DLIC2 (1:200; gifts from M. McCaffrey, Biosciences Institute, University College Cork, Cork, Ireland), anti-H2AX (1:1,000; EMD Millipore), anti-ARP1 (1:2,000; a gift from T. Schroer, Johns Hopkins University, Baltimore, MD), anti-Spindly (1:2,500; Bethyl Laboratories, Inc.), and anti-BICD2 (1:1,000; a gift from A. Akhmanova, Utrecht University, Utrecht, Netherlands). HRP-coupled secondary antibodies (Dako) were used in a 1:2,500 dilution. The immunopositive bands were visualized using ECL Western blotting reagent (GE Healthcare).

Online supplemental material

Fig. S1 A shows the mitotic index in U2OS cells upon depletion of the complete siRNA collection. Fig. S1 B shows an example of a cell with chromosome scattering after a prolonged mitosis. Fig. S2 contains validation experiments for centrosome positioning, spindle pole focusing, and the Eg5-antagonism assay in a different cell line. Fig. S3 shows that dynactin-depleted cells do not retain checkpoint proteins at their kinetochores upon chromosome alignment. Fig. S4 shows the localization of KT-dynein in the presence of microtubules. Fig. S5 shows that dynactin depletion leads to reduced dynein at the spindle poles. Table S1 gives an overview of all the genes that were included in the siRNA library. Table S2 lists all primers that were used for the qRT-PCR analysis. Online supplemental material is available at http://www.jcb.org/cgi/content/full/jcb.201208098/DC1.

We thank A. Akhmanova for sharing reagents and experimental help. We would like to thank B. van den Broek for technical assistance with the microscopes. Furthermore, we would like to thank G. Kops for sharing reagents. We would like to thank O. Reiner for the LIS1 antibody, M. McCaffrey for the DLIC1 and DLIC2 antibodies, A. Musacchio for the MAD1 antibody, and T. Schroer for the ARP1 antibody. We would like to thank T. Hyman for the HeLa cells stably expressing the BAC plasmid encoding GFP-tagged dynein heavy chain. Finally, we would like to thank A. Janssen and R. van Heesbeen for critically reading this manuscript.

This work was supported by the Netherlands Genomic Initiative of NWO and a ZonMW TOP project (40-00812-98-10021) to R.H. Medema.

Submitted: 16 August 2012
Accepted: 18 March 2013

References

Amaro, I.A., M. Costanzo, C. Boone, and T.C. Huffaker. 2008. The *Saccharomyces cerevisiae* homolog of p24 is essential for maintaining the association of p150Glued with the dynactin complex. *Genetics*. 178:703–709. http://dx.doi.org/10.1534/genetics.107.079103

Blangy, A., H.A. Lane, P. d'Hérin, M. Harper, M. Kress, and E.A. Nigg. 1995. Phosphorylation by p34cdc2 regulates spindle association of human Eg5, a kinesin-related motor essential for bipolar spindle formation in vivo. *Cell*. 83:1159–1169. http://dx.doi.org/10.1016/0092-8674(95)90142-6

Bolhy, S., I. Bouhlel, E. Dultz, T. Nayak, M. Zuccolo, X. Gatti, R. Vallee, J. Ellenberg, and V. Doye. 2011. A Nup133-dependent NPC-anchored network tethers centrosomes to the nuclear envelope in prophase. *J. Cell Biol.* 192:855–871. http://dx.doi.org/10.1083/jcb.201007118

Burkhardt, J.K., C.J. Echeverri, T. Nilsson, and R.B. Vallee. 1997. Overexpression of the dynamitin (p50) subunit of the dynactin complex disrupts dynein-dependent maintenance of membrane organelle distribution. *J. Cell Biol.* 139:469–484. http://dx.doi.org/10.1083/jcb.139.2.469

Crackower, M.A., D.S. Sinasac, J. Xia, J. Motoyama, M. Prochazka, J.M. Rommens, S.W. Scherer, and L.C. Tsui. 1999. Cloning and characterization of two cytoplasmic dynein intermediate chain genes in mouse and human. *Genomics*. 55:257–267. http://dx.doi.org/10.1006/geno.1998.5665

Culver-Hanlon, T.L., S.A. Lex, A.D. Stephens, N.J. Quintyne, and S.J. King. 2006. A microtubule-binding domain in dynactin increases dynein processivity by skating along microtubules. *Nat. Cell Biol.* 8:264–270. http://dx.doi.org/10.1038/ncb1370

Daum, J.R., T.A. Potapova, S. Sivakumar, J.J. Daniel, J.N. Flynn, S. Rankin, and G.J. Gorbsky. 2011. Cohesion fatigue induces chromatid separation in cells delayed at metaphase. *Curr. Biol.* 21:1018–1024. http://dx.doi.org/10.1016/j.cub.2011.05.032

DeBonis, S., D.A. Skoufias, L. Lebeau, R. Lopez, G. Robin, R.L. Margolis, R.H. Wade, and F. Kozielski. 2004. In vitro screening for inhibitors of the human mitotic kinesin Eg5 with antimitotic and antitumor activities. *Mol. Cancer Ther.* 3:1079–1090.

Dujardin, D.L., and R.B. Vallee. 2002. Dynein at the cortex. *Curr. Opin. Cell Biol.* 14:44–49. http://dx.doi.org/10.1016/S0955-0674(01)00292-7

Echeverri, C.J., B.M. Paschal, K.T. Vaughan, and R.B. Vallee. 1996. Molecular characterization of the 50-kD subunit of dynactin reveals function for the complex in chromosome alignment and spindle organization during mitosis. *J. Cell Biol.* 132:617–633. http://dx.doi.org/10.1083/jcb.132.4.617

Eckley, D.M., S.R. Gill, K.A. Melkonian, J.B. Bingham, H.V. Goodson, J.E. Heuser, and T.A. Schroer. 1999. Analysis of dynactin subcomplexes reveals a novel actin-related protein associated with the arp1 minifilament pointed end. *J. Cell Biol.* 147:307–320. http://dx.doi.org/10.1083/jcb.147.2.307

Egan, M.J., K. Tan, and S.L. Reck-Peterson. 2012. Lis1 is an initiation factor for dynein-driven organelle transport. *J. Cell Biol.* 197:971–982. http://dx.doi.org/10.1083/jcb.201112101

Faulkner, N.E., D.L. Dujardin, C.Y. Tai, K.T. Vaughan, C.B. O'Connell, Y. Wang, and R.B. Vallee. 2000. A role for the lissencephaly gene LIS1 in mitosis and cytoplasmic dynein function. *Nat. Cell Biol.* 2:784–791. http://dx.doi.org/10.1038/35041020

Ferenz, N.P., R. Paul, C. Fagerstrom, A. Mogilner, and P. Wadsworth. 2009. Dynein antagonizes eg5 by crosslinking and sliding antiparallel microtubules. *Curr. Biol.* 19:1833–1838. http://dx.doi.org/10.1016/j.cub.2009.09.025

Gassmann, R., A. Essex, J.S. Hu, P.S. Maddox, F. Motegi, A. Sugimoto, S.M. O'Rourke, B. Bowerman, I. McLeod, J.R. Yates III, et al. 2008. A new mechanism controlling kinetochore-microtubule interactions revealed by comparison of two dynein-targeting components: SPDL-1 and the Rod/Zwilch/Zw10 complex. *Genes Dev.* 22:2385–2399. http://dx.doi.org/10.1101/gad.1687508

Gassmann, R., A.J. Holland, D. Varma, X. Wan, F. Civril, D.W. Cleveland, K. Oegema, E.D. Salmon, and A. Desai. 2010. Removal of Spindly from microtubule-attached kinetochores controls spindle checkpoint silencing in human cells. *Genes Dev.* 24:957–971. http://dx.doi.org/10.1101/gad.1886810

Gill, S.R., T.A. Schroer, I. Szilak, E.R. Steuer, M.P. Sheetz, and D.W. Cleveland. 1991. Dynactin, a conserved, ubiquitously expressed component of an

activator of vesicle motility mediated by cytoplasmic dynein. *J. Cell Biol.* 115:1639–1650. http://dx.doi.org/10.1083/jcb.115.6.1639

Gönczy, P., S. Pichler, M. Kirkham, and A.A. Hyman. 1999. Cytoplasmic dynein is required for distinct aspects of MTOC positioning, including centrosome separation, in the one cell stage *Caenorhabditis elegans* embryo. *J. Cell Biol.* 147:135–150. http://dx.doi.org/10.1083/jcb.147.1.135

Goshima, G., F. Nédélec, and R.D. Vale. 2005. Mechanisms for focusing mitotic spindle poles by minus end-directed motor proteins. *J. Cell Biol.* 171:229–240. http://dx.doi.org/10.1083/jcb.200505107

Griffis, E.R., N. Stuurman, and R.D. Vale. 2007. Spindly, a novel protein essential for silencing the spindle assembly checkpoint, recruits dynein to the kinetochore. *J. Cell Biol.* 177:1005–1015. http://dx.doi.org/10.1083/jcb.200702062

Hagan, R.S., M.S. Manak, H.K. Buch, M.G. Meier, P. Meraldi, J.V. Shah, and P.K. Sorger. 2011. p31(comet) acts to ensure timely spindle checkpoint silencing subsequent to kinetochore attachment. *Mol. Biol. Cell*. 22:4236–4246. http://dx.doi.org/10.1091/mbc.E11-03-0216

Hall, J., Y. Song, P.A. Karplus, and E. Barbar. 2010. The crystal structure of dynein intermediate chain-light chain roadblock complex gives new insights into dynein assembly. *J. Biol. Chem.* 285:22566–22575. http://dx.doi.org/10.1074/jbc.M110.103861

Heald, R., R. Tournebize, T. Blank, R. Sandaltzopoulos, P. Becker, A. Hyman, and E. Karsenti. 1996. Self-organization of microtubules into bipolar spindles around artificial chromosomes in *Xenopus* egg extracts. *Nature*. 382:420–425. http://dx.doi.org/10.1038/382420a0

Holleran, E.A., L.A. Ligon, M. Tokito, M.C. Stankewich, J.S. Morrow, and E.L. Holzbaur. 2001. beta III spectrin binds to the Arp1 subunit of dynactin. *J. Biol. Chem.* 276:36598–36605. http://dx.doi.org/10.1074/jbc.M104838200

Howell, B.J., B.F. McEwen, J.C. Canman, D.B. Hoffman, E.M. Farrar, C.L. Rieder, and E.D. Salmon. 2001. Cytoplasmic dynein/dynactin drives kinetochore protein transport to the spindle poles and has a role in mitotic spindle checkpoint inactivation. *J. Cell Biol.* 155:1159–1172. http://dx.doi.org/10.1083/jcb.200105093

Huang, J., A.J. Roberts, A.E. Leschziner, and S.L. Reck-Peterson. 2012. Lis1 acts as a "clutch" between the ATPase and microtubule-binding domains of the dynein motor. *Cell*. 150:975–986. http://dx.doi.org/10.1016/j.cell.2012.07.022

Jacquot, G., P. Maidou-Peindara, and S. Benichou. 2010. Molecular and functional basis for the scaffolding role of the p50/dynamitin subunit of the microtubule-associated dynactin complex. *J. Biol. Chem.* 285:23019–23031. http://dx.doi.org/10.1074/jbc.M110.100602

Johansson, M., N. Rocha, W. Zwart, I. Jordens, L. Janssen, C. Kuijl, V.M. Olkkonen, and J. Neefjes. 2007. Activation of endosomal dynein motors by stepwise assembly of Rab7-RILP-p150Glued, ORP1L, and the receptor betalll spectrin. *J. Cell Biol.* 176:459–471. http://dx.doi.org/10.1083/jcb.200606077

Kapitein, L.C., E.J. Peterman, B.H. Kwok, J.H. Kim, T.M. Kapoor, and C.F. Schmidt. 2005. The bipolar mitotic kinesin Eg5 moves on both microtubules that it crosslinks. *Nature*. 435:114–118. http://dx.doi.org/10.1038/nature03503

Kardon, J.R., and R.D. Vale. 2009. Regulators of the cytoplasmic dynein motor. *Nat. Rev. Mol. Cell Biol.* 10:854–865. http://dx.doi.org/10.1038/nrm2804

Kardon, J.R., S.L. Reck-Peterson, and R.D. Vale. 2009. Regulation of the processivity and intracellular localization of *Saccharomyces cerevisiae* dynein by dynactin. *Proc. Natl. Acad. Sci. USA*. 106:5669–5674. http://dx.doi.org/10.1073/pnas.0900976106

Karki, S., and E.L. Holzbaur. 1999. Cytoplasmic dynein and dynactin in cell division and intracellular transport. *Curr. Opin. Cell Biol.* 11:45–53. http://dx.doi.org/10.1016/S0955-0674(99)80006-4

Kashina, A.S., R.J. Baskin, D.G. Cole, K.P. Wedaman, W.M. Saxton, and J.M. Scholey. 1996. A bipolar kinesin. *Nature*. 379:270–272. http://dx.doi.org/10.1038/379270a0

King, S.J., and T.A. Schroer. 2000. Dynactin increases the processivity of the cytoplasmic dynein motor. *Nat. Cell Biol.* 2:20–24. http://dx.doi.org/10.1038/71338

Kiyomitsu, T., and I.M. Cheeseman. 2012. Chromosome- and spindle-pole-derived signals generate an intrinsic code for spindle position and orientation. *Nat. Cell Biol.* 14:311–317. http://dx.doi.org/10.1038/ncb2440

Kwiatkowski, N., N. Jelluma, P. Filippakopoulos, M. Soundararajan, M.S. Manak, M. Kwon, H.G. Choi, T. Sim, Q.L. Deveraux, S. Rottmann, et al. 2010. Small-molecule kinase inhibitors provide insight into Mps1 cell cycle function. *Nat. Chem. Biol.* 6:359–368. http://dx.doi.org/10.1038/nchembio.345

Lenz, J.H., I. Schuchardt, A. Straube, and G. Steinberg. 2006. A dynein loading zone for retrograde endosome motility at microtubule plus-ends. *EMBO J.* 25:2275–2286. http://dx.doi.org/10.1038/sj.emboj.7601119

Li, J., W.L. Lee, and J.A. Cooper. 2005. NudEL targets dynein to microtubule ends through LIS1. *Nat. Cell Biol.* 7:686–690. http://dx.doi.org/10.1038/ncb1273

Liang, Y., W. Yu, Y. Li, L. Yu, Q. Zhang, F. Wang, Z. Yang, J. Du, Q. Huang, X. Yao, and X. Zhu. 2007. Nudel modulates kinetochore association and function of cytoplasmic dynein in M phase. *Mol. Biol. Cell*. 18:2656–2666. http://dx.doi.org/10.1091/mbc.E06-04-0345

McKenney, R.J., M. Vershinin, A. Kunwar, R.B. Vallee, and S.P. Gross. 2010. LIS1 and NudE induce a persistent dynein force-producing state. *Cell*. 141:304–314. http://dx.doi.org/10.1016/j.cell.2010.02.035

McKenney, R.J., S.J. Weil, J. Scherer, and R.B. Vallee. 2011. Mutually exclusive cytoplasmic dynein regulation by NudE-Lis1 and dynactin. *J. Biol. Chem.* 286:39615–39622. http://dx.doi.org/10.1074/jbc.M111.289017

Melkonian, K.A., K.C. Maier, J.E. Godfrey, M. Rodgers, and T.A. Schroer. 2007. Mechanism of dynamitin-mediated disruption of dynactin. *J. Biol. Chem.* 282:19355–19364. http://dx.doi.org/10.1074/jbc.M700003200

Mikami, A., S.H. Tynan, T. Hama, K. Luby-Phelps, T. Saito, J.E. Crandall, J.C. Besharse, and R.B. Vallee. 2002. Molecular structure of cytoplasmic dynein 2 and its distribution in neuronal and ciliated cells. *J. Cell Sci.* 115:4801–4808. http://dx.doi.org/10.1242/jcs.00168

Mitchison, T.J., P. Maddox, J. Gaetz, A. Groen, M. Shirasu, A. Desai, E.D. Salmon, and T.M. Kapoor. 2005. Roles of polymerization dynamics, opposed motors, and a tensile element in governing the length of *Xenopus* extract meiotic spindles. *Mol. Biol. Cell*. 16:3064–3076. http://dx.doi.org/10.1091/mbc.E05-02-0174

Muresan, V., M.C. Stankewich, W. Steffen, J.S. Morrow, E.L. Holzbaur, and B.J. Schnapp. 2001. Dynactin-dependent, dynein-driven vesicle transport in the absence of membrane proteins: a role for spectrin and acidic phospholipids. *Mol. Cell*. 7:173–183. http://dx.doi.org/10.1016/S1097-2765(01)00165-4

Nyarko, A., Y. Song, and E. Barbar. 2012. Intrinsic disorder in dynein intermediate chain modulates its interactions with NudE and dynactin. *J. Biol. Chem.* 287:24884–24893. http://dx.doi.org/10.1074/jbc.M112.376038

Palmer, K.J., H. Hughes, and D.J. Stephens. 2009. Specificity of cytoplasmic dynein subunits in discrete membrane-trafficking steps. *Mol. Biol. Cell*. 20:2885–2899. http://dx.doi.org/10.1091/mbc.E08-12-1160

Pfarr, C.M., M. Coue, P.M. Grissom, T.S. Hays, M.E. Porter, and J.R. McIntosh. 1990. Cytoplasmic dynein is localized to kinetochores during mitosis. *Nature*. 345:263–265. http://dx.doi.org/10.1038/345263a0

Pfister, K.K., P.R. Shah, H. Hummerich, A. Russ, J. Cotton, A.A. Annuar, S.M. King, and E.M. Fisher. 2006. Genetic analysis of the cytoplasmic dynein subunit families. *PLoS Genet.* 2:e1. http://dx.doi.org/10.1371/journal.pgen.0020001

Poser, I., M. Sarov, J.R. Hutchins, J.K. Hériché, Y. Toyoda, A. Pozniakovsky, D. Weigl, A. Nitzsche, B. Hegemann, A.W. Bird, et al. 2008. BAC TransgeneOmics: a high-throughput method for exploration of protein function in mammals. *Nat. Methods*. 5:409–415. http://dx.doi.org/10.1038/nmeth.1199

Quintyne, N.J., S.R. Gill, D.M. Eckley, C.L. Crego, D.A. Compton, and T.A. Schroer. 1999. Dynactin is required for microtubule anchoring at centrosomes. *J. Cell Biol.* 147:321–334. http://dx.doi.org/10.1083/jcb.147.2.321

Raaijmakers, J.A., M.E. Tanenbaum, A.F. Maia, and R.H. Medema. 2009. RAMA1 is a novel kinetochore protein involved in kinetochore-microtubule attachment. *J. Cell Sci.* 122:2436–2445. http://dx.doi.org/10.1242/jcs.051912

Raaijmakers, J.A., R.G. van Heesbeen, J.L. Meaders, E.F. Geers, B. Fernandez-Garcia, R.H. Medema, and M.E. Tanenbaum. 2012. Nuclear envelope-associated dynein drives prophase centrosome separation and enables Eg5-independent bipolar spindle formation. *EMBO J.* 31:4179–4190. http://dx.doi.org/10.1038/emboj.2012.272

Robinson, J.T., E.J. Wojcik, M.A. Sanders, M. McGrail, and T.S. Hays. 1999. Cytoplasmic dynein is required for the nuclear attachment and migration of centrosomes during mitosis in *Drosophila*. *J. Cell Biol.* 146:597–608. http://dx.doi.org/10.1083/jcb.146.3.597

Salina, D., K. Bodoor, D.M. Eckley, T.A. Schroer, J.B. Rattner, and B. Burke. 2002. Cytoplasmic dynein as a facilitator of nuclear envelope breakdown. *Cell*. 108:97–107. http://dx.doi.org/10.1016/S0092-8674(01)00628-6

Sawin, K.E., K. LeGuellec, M. Philippe, and T.J. Mitchison. 1992. Mitotic spindle organization by a plus-end-directed microtubule motor. *Nature*. 359:540–543. http://dx.doi.org/10.1038/359540a0

Schmidt, J.C., T. Kiyomitsu, T. Hori, C.B. Backer, T. Fukagawa, and I.M. Cheeseman. 2010. Aurora B kinase controls the targeting of the Astrin-SKAP complex to bioriented kinetochores. *J. Cell Biol.* 191:269–280. http://dx.doi.org/10.1083/jcb.201006129

Schroer, T.A. 2004. Dynactin. *Annu. Rev. Cell Dev. Biol.* 20:759–779. http://dx.doi.org/10.1146/annurev.cellbio.20.012103.094623

Schroer, T.A., and M.P. Sheetz. 1991. Two activators of microtubule-based vesicle transport. *J. Cell Biol.* 115:1309–1318. http://dx.doi.org/10.1083/jcb.115.5.1309

Sharp, D.J., G.C. Rogers, and J.M. Scholey. 2000. Cytoplasmic dynein is required for poleward chromosome movement during mitosis in *Drosophila* embryos. *Nat. Cell Biol.* 2:922–930. http://dx.doi.org/10.1038/35046574

Song, J., R.C. Tyler, M.S. Lee, E.M. Tyler, and J.L. Markley. 2005. Solution structure of isoform 1 of Roadblock/LC7, a light chain in the dynein complex. *J. Mol. Biol.* 354:1043–1051. http://dx.doi.org/10.1016/j.jmb.2005.10.017

Splinter, D., M.E. Tanenbaum, A. Lindqvist, D. Jaarsma, A. Flotho, K.L. Yu, I. Grigoriev, D. Engelsma, E.D. Haasdijk, N. Keijzer, et al. 2010. Bicaudal D2, dynein, and kinesin-1 associate with nuclear pore complexes and regulate centrosome and nuclear positioning during mitotic entry. *PLoS Biol.* 8:e1000350. http://dx.doi.org/10.1371/journal.pbio.1000350

Splinter, D., D.S. Razafsky, M.A. Schlager, A. Serra-Marques, I. Grigoriev, J. Demmers, N. Keijzer, K. Jiang, I. Poser, A.A. Hyman, et al. 2012. BICD2, dynactin, and LIS1 cooperate in regulating dynein recruitment to cellular structures. *Mol. Biol. Cell*. 23:4226–4241. http://dx.doi.org/10.1091/mbc.E12-03-0210

Starr, D.A., B.C. Williams, T.S. Hays, and M.L. Goldberg. 1998. ZW10 helps recruit dynactin and dynein to the kinetochore. *J. Cell Biol.* 142:763–774. http://dx.doi.org/10.1083/jcb.142.3.763

Stehman, S.A., Y. Chen, R.J. McKenney, and R.B. Vallee. 2007. NudE and NudEL are required for mitotic progression and are involved in dynein recruitment to kinetochores. *J. Cell Biol.* 178:583–594. http://dx.doi.org/10.1083/jcb.200610112

Steuer, E.R., L. Wordeman, T.A. Schroer, and M.P. Sheetz. 1990. Localization of cytoplasmic dynein to mitotic spindles and kinetochores. *Nature*. 345:266–268. http://dx.doi.org/10.1038/345266a0

Stevens, D., R. Gassmann, K. Oegema, and A. Desai. 2011. Uncoordinated loss of chromatid cohesion is a common outcome of extended metaphase arrest. *PLoS ONE*. 6:e22969. http://dx.doi.org/10.1371/journal.pone.0022969

Susalka, S.J., K. Nikulina, M.W. Salata, P.S. Vaughan, S.M. King, K.T. Vaughan, and K.K. Pfister. 2002. The roadblock light chain binds a novel region of the cytoplasmic Dynein intermediate chain. *J. Biol. Chem.* 277:32939–32946. http://dx.doi.org/10.1074/jbc.M205510200

Tai, A.W., J.Z. Chuang, C. Bode, U. Wolfrum, and C.H. Sung. 1999. Rhodopsin's carboxy-terminal cytoplasmic tail acts as a membrane receptor for cytoplasmic dynein by binding to the dynein light chain Tctex-1. *Cell*. 97:877–887. http://dx.doi.org/10.1016/S0092-8674(00)80800-4

Tai, C.Y., D.L. Dujardin, N.E. Faulkner, and R.B. Vallee. 2002. Role of dynein, dynactin, and CLIP-170 interactions in LIS1 kinetochore function. *J. Cell Biol.* 156:959–968. http://dx.doi.org/10.1083/jcb.200109046

Tanenbaum, M.E., L. Macůrek, N. Galjart, and R.H. Medema. 2008. Dynein, Lis1 and CLIP-170 counteract Eg5-dependent centrosome separation during bipolar spindle assembly. *EMBO J.* 27:3235–3245. http://dx.doi.org/10.1038/emboj.2008.242

Tanenbaum, M.E., L. Macůrek, A. Janssen, E.F. Geers, M. Alvarez-Fernández, and R.H. Medema. 2009. Kif15 cooperates with eg5 to promote bipolar spindle assembly. *Curr. Biol.* 19:1703–1711. http://dx.doi.org/10.1016/j.cub.2009.08.027

Tanenbaum, M.E., A. Akhmanova, and R.H. Medema. 2010. Dynein at the nuclear envelope. *EMBO Rep.* 11:649. http://dx.doi.org/10.1038/embor.2010.127

Tynan, S.H., A. Purohit, S.J. Doxsey, and R.B. Vallee. 2000. Light intermediate chain 1 defines a functional subfraction of cytoplasmic dynein which binds to pericentrin. *J. Biol. Chem.* 275:32763–32768. http://dx.doi.org/10.1074/jbc.M001536200

Vaisberg, E.A., M.P. Koonce, and J.R. McIntosh. 1993. Cytoplasmic dynein plays a role in mammalian mitotic spindle formation. *J. Cell Biol.* 123:849–858. http://dx.doi.org/10.1083/jcb.123.4.849

Vanneste, D., M. Takagi, N. Imamoto, and I. Vernos. 2009. The role of Hklp2 in the stabilization and maintenance of spindle bipolarity. *Curr. Biol.* 19:1712–1717. http://dx.doi.org/10.1016/j.cub.2009.09.019

Varma, D., P. Monzo, S.A. Stehman, and R.B. Vallee. 2008. Direct role of dynein motor in stable kinetochore-microtubule attachment, orientation, and alignment. *J. Cell Biol.* 182:1045–1054. http://dx.doi.org/10.1083/jcb.200710106

Vassilev, L.T., C. Tovar, S. Chen, D. Knezevic, X. Zhao, H. Sun, D.C. Heimbrook, and L. Chen. 2006. Selective small-molecule inhibitor reveals critical mitotic functions of human CDK1. *Proc. Natl. Acad. Sci. USA*. 103:10660–10665. http://dx.doi.org/10.1073/pnas.0600447103

Vaughan, K.T., and R.B. Vallee. 1995. Cytoplasmic dynein binds dynactin through a direct interaction between the intermediate chains and p150Glued. *J. Cell Biol.* 131:1507–1516. http://dx.doi.org/10.1083/jcb.131.6.1507

Verde, F., J.M. Berrez, C. Antony, and E. Karsenti. 1991. Taxol-induced microtubule asters in mitotic extracts of *Xenopus* eggs: requirement for phosphorylated factors and cytoplasmic dynein. *J. Cell Biol.* 112:1177–1187. http://dx.doi.org/10.1083/jcb.112.6.1177

Vergnolle, M.A., and S.S. Taylor. 2007. Cenp-F links kinetochores to Ndel1/Nde1/Lis1/dynein microtubule motor complexes. *Curr. Biol.* 17:1173–1179. http://dx.doi.org/10.1016/j.cub.2007.05.077

Waterman-Storer, C.M., S. Karki, and E.L. Holzbaur. 1995. The p150Glued component of the dynactin complex binds to both microtubules and the actin-related protein centractin (Arp-1). *Proc. Natl. Acad. Sci. USA*. 92:1634–1638. http://dx.doi.org/10.1073/pnas.92.5.1634

Whyte, J., J.R. Bader, S.B. Tauhata, M. Raycroft, J. Hornick, K.K. Pfister, W.S. Lane, G.K. Chan, E.H. Hinchcliffe, P.S. Vaughan, and K.T. Vaughan. 2008. Phosphorylation regulates targeting of cytoplasmic dynein to kinetochores during mitosis. *J. Cell Biol.* 183:819–834. http://dx.doi.org/10.1083/jcb.200804114

Wittmann, T., and T. Hyman. 1999. Recombinant p50/dynamitin as a tool to examine the role of dynactin in intracellular processes. *Methods Cell Biol.* 61:137–143. http://dx.doi.org/10.1016/S0091-679X(08)61978-0

Wojcik, E., R. Basto, M. Serr, F. Scaërou, R. Karess, and T. Hays. 2001. Kinetochore dynein: its dynamics and role in the transport of the Rough deal checkpoint protein. *Nat. Cell Biol.* 3:1001–1007. http://dx.doi.org/10.1038/ncb1101-1001

Yamada, M., S. Toba, Y. Yoshida, K. Haratani, D. Mori, Y. Yano, Y. Mimori-Kiyosue, T. Nakamura, K. Itoh, S. Fushiki, et al. 2008. LIS1 and NDEL1 coordinate the plus-end-directed transport of cytoplasmic dynein. *EMBO J.* 27:2471–2483. http://dx.doi.org/10.1038/emboj.2008.182

Zhang, J., G. Han, and X. Xiang. 2002. Cytoplasmic dynein intermediate chain and heavy chain are dependent upon each other for microtubule end localization in Aspergillus nidulans. *Mol. Microbiol.* 44:381–392. http://dx.doi.org/10.1046/j.1365-2958.2002.02900.x

Zyłkiewicz, E., M. Kijańska, W.C. Choi, U. Derewenda, Z.S. Derewenda, and P.T. Stukenberg. 2011. The N-terminal coiled-coil of Ndel1 is a regulated scaffold that recruits LIS1 to dynein. *J. Cell Biol.* 192:433–445. http://dx.doi.org/10.1083/jcb.201011142